Flow-focused synthesis of monodisperse gold nanoparticles using ionic liquids on a microfluidic platform†

Laura L. Lazarus,[a] Astro S.-J. Yang,[b] Steven Chu,[b] Richard L. Brutchey*[a] and Noah Malmstadt*[b]

Received 14th August 2010, Accepted 14th October 2010
DOI: 10.1039/c0lc00297f

A microfluidic device was used in tandem with an imidazolium-based ionic liquid to fabricate monodisperse gold nanoparticles (4.38 ± 0.53 nm) with excellent control over size and morphology.

As novel applications for nanoparticles continue to emerge, there is an increasing need for approaches to nanomanufacture these materials using inexpensive, rapid, and reproducible methods that have minimal impact on the environment.[1] Microfluidic devices are being explored as one possible way to nanomanufacture nanoparticles with control over the size, size distribution, and crystal phase of the resulting particles.[2] Such control is made possible by improved heat and mass transport within the microfluidic channels that result from high surface area-to-volume ratios, in addition to fast reagent mixing. Moreover, microfluidic devices allow for reduction of environmental risks associated with nanofabrication by allowing small-volume, on-demand syntheses that also result in higher yields and less by-product generation.[3]

Gold nanoparticles (AuNPs) possess size- and shape-dependent optical properties that are a direct result of the surface plasmon resonance, which make them useful in a wide range of applications from bionanotechnology to chemical catalysis.[4] In the typical batch reaction, AuNPs are prepared by the reduction of a Au(III) salt in the presence of stabilizing ligands, such as thiols or quaternary ammonium salts.[5] Recently, imidazolium-based ionic liquids (ILs) have demonstrated promise as a dual-function solvent system and stabilizing ligand for metal nanoparticles.[6] ILs are promising solvents for synthetic reactions in poly(dimethylsiloxane) (PDMS) microfluidic devices since they do not suffer from the PDMS incompatibility that limits the use of traditional organic solvents.[7] Moreover, ILs are non-flammable and possess negligible vapor pressures, in addition to having the ability to stabilize metal nanoparticles because of their high ionic charge, high dielectric constant, and ability to form supramolecular hydrogen-bonded networks in the condensed phase, which may serve as structure directing networks for nanoparticle growth.[6] As such, in the past few years there have been a number of examples of AuNPs being synthesized in imidazolium-based ILs;[8] however, the resulting nanoparticles tend to have relatively polydisperse size distributions. Herein, we describe the synthesis of small, monodisperse AuNPs using the beneficial properties inherent to both controlled (and rapid) microfluidic mixing and imidazolium-based ILs.

In a typical procedure, solutions of tetrachloroauric acid hydrate ($HAuCl_4 \cdot 3H_2O$, 10 mM; 99.9%, Strem Chemicals), sodium borohydride ($NaBH_4$, 100 mM; 99%, Sigma-Aldrich) and 1-methylimidazole (~4.9 M; 99%, Alfa Aesar) were prepared in 1-butyl-3-methylimidazolium tetrafluoroborate (BMIM-BF_4; 98+%, Alfa Aesar) by stirring under ambient conditions until the reagents were fully dissolved. The 1-methylimidazole, which is a common impurity in imidazolium-based ILs, is thought to stabilize and perhaps slow the growth of AuNPs and is used here as a weakly coordinating stabilizing ligand.[8a] Prior to injection into the microfluidic device, the $HAuCl_4$ and 1-methylimidazole solutions were combined (1 : 1, v/v) with stirring for *ca.* 15 min.

The microfluidic device was fabricated through a standard photolithography process and consists of a cast PDMS layer bonded to a bare PDMS substrate (see ESI†). The device measures 3 × 5 cm overall and the channel widths and depths are 600 and 95 μm, respectively, with a total channel volume of 7.6 μL. Before use, the device was silanized with trichloro(1*H*,1*H*,2*H*,2*H*-perfluorooctyl)silane (97%, Sigma-Aldrich) for 20 min to make the channel surface hydrophobic and prevent device fouling by AuNP adsorption on the channel walls.[2c] A stream of pure BMIM-BF_4 was injected between the two reagent streams ($HAuCl_4$/1-methylimidazole and $NaBH_4$ in BMIM-BF_4) to insure that reagent mixing occurred only by interdiffusion between laminar streams. This pure BMIM-BF_4 stream and the two reagent streams were injected by syringe pump at a flow rate ratio of 5 : 9 : 9 *via* inlets I, II, and III, respectively (Fig. 1). An inert polychlorotrifluoroethylene oil (Halocarbon 6.3 oil; River Edge, NJ) was introduced *via* inlet V at a flow rate of either 2070 μL h^{-1} or 7000 μL h^{-1}. These inert oil flow rates defined two flow regimes—at the lower flow rate, the central IL stream remained continuous through the device while at the higher flow rate it broke up into droplets (the transition between flow regimes occurred at an inert oil flow rate of about 3000 μL h^{-1}; see ESI†). The reaction products were collected continuously from outlet IV and quenched/precipitated into a reservoir containing ethanol.

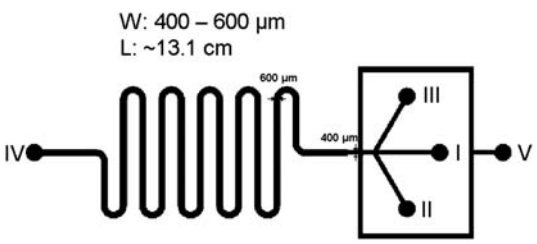

Fig. 1 Schematic representation of the microfluidic device used to fabricate monodisperse AuNPs.

[a]*Department of Chemistry, University of Southern California, Los Angeles, CA, 90089, USA. E-mail: brutchey@usc.edu*
[b]*Mork Family Department of Chemical Engineering and Materials Science, University of Southern California, Los Angeles, CA, 90089, USA. E-mail: malmstad@usc.edu*

† Electronic supplementary information (ESI) available: Experimental details, photograph of device and droplet flow, and additional TEM micrographs. See DOI: 10.1039/c0lc00297f

The AuNPs were isolated by centrifugation (6000 rpm, 5 min) followed by washing twice with fresh ethanol to remove excess BMIM-BF_4. The isolated AuNPs were redispersed in hexanes and 1-dodecanethiol (5–10 μL mL^{-1} hexanes) by sonication, which gave red suspensions that were stable for months. The resulting AuNPs were analyzed by powder X-ray diffraction (XRD), selected area electron diffraction (SAED) and UV-vis spectroscopy. The size, morphology, and size distribution of the resulting AuNPs were characterized by transmission electron microscopy (TEM).

Using this device configuration, the AuNPs obtained with the higher, droplet-forming inert oil flow rate were monodisperse with a mean diameter of 4.38 ± 0.53 nm (σ/μ_d = 12.1%), as determined by TEM analysis (Fig. 2a). These particles were overwhelmingly spherical with only 15.0% having a roundness, defined as (4 × particle area)/[π × (major axis length)²], less than 0.85. UV-vis spectra of the deep red AuNP suspensions gave relatively narrow surface plasmon bands centered at λ = 518.5 nm, typical of AuNPs that are largely non-agglomerated (see ESI† for comparison to a broadened and red-shifted surface plasmon band for agglomerated AuNPs).[9] The XRD pattern of the AuNPs can be assigned to the face centered cubic (fcc) structure of gold (JCPDS no. 04-0784), with a lattice parameter of a = 4.07 Å that matches literature values. The crystallinity of the AuNPs was further confirmed by SAED analysis. The diffuse diffraction rings produced by an ensemble of nanoparticles were indexed to the characteristic {111}, {200}, {220}, and {311} diffraction planes of fcc gold (inset, Fig. 3), and the lattice parameter corroborates that calculated by powder XRD. Energy dispersive X-ray spectroscopic analysis suggests that the majority of the 1-methylimidazole and BMIM-BF_4 is displaced from the AuNP surface upon work-up with thiol, with the analyses for nitrogen and fluorine giving baseline integrated signal relative to that of sulfur (see ESI†).

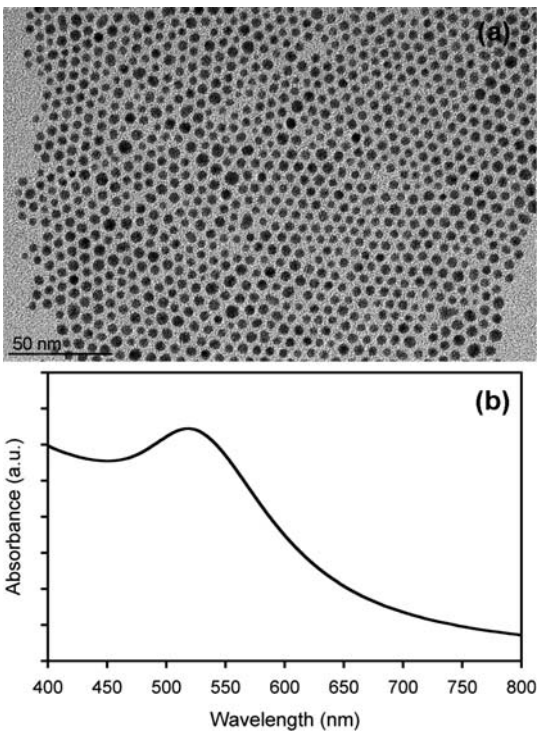

Fig. 2 (a) TEM micrograph of AuNPs obtained under droplet flow in the microfluidic device and (b) representative UV-vis spectrum of AuNPs exhibiting the characteristic surface plasmon band (λ_{max} = 518.5 nm).

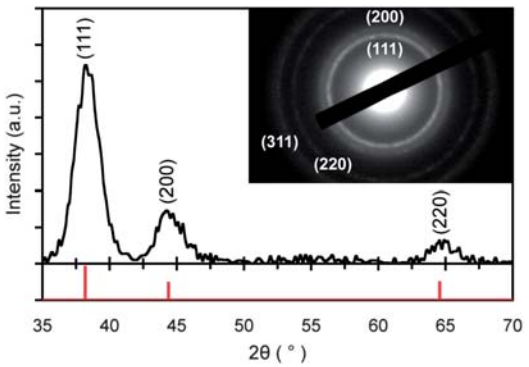

Fig. 3 Powder XRD pattern of AuNPs indexed to fcc gold. Inset: characteristic SAED pattern confirming crystalline AuNPs.

Flow focusing by inert carrier oil has a dramatic effect on the size and morphological fidelity of the AuNPs. When the flow rate of the inert oil is decreased such that the IL stream no longer forms droplets, particles are larger (5.65 ± 1.03 nm) and more polydisperse (σ/μ_d = 18.2%) (see ESI†). They were also less spherical, with 23.4% having a roundness less than 0.85. In either flow-focused device geometry, the inert oil forces the two reagent streams, and the center BMIM-BF_4 stream separating them, down to narrower widths. As a result, the diffusion lengths needed for the two reagents to mix in the center BMIM-BF_4 stream are reduced. To illustrate the importance of flow focusing, an analogous microfluidic device was constructed without the additional carrier oil inlet (*i.e.*, inlet V in Fig. 1). The three streams of BMIM-BF_4, $HAuCl_4$/1-methylimidazole, and $NaBH_4$ were introduced *via* syringe pump at flow rates of 500, 900, and 900 μL h^{-1} through inlets I, II, and III, respectively. Laminar flow is observed under these conditions, with AuNP formation discernible further down channel as the center stream turns purple in color. Using this laminar flow device configuration, the AuNPs are more polydisperse and have a larger mean diameter (6.25 ± 1.29 nm; σ/μ_d = 20.6%), in addition to being more spheroidal in shape with 28.2% having a roundness less than 0.85 (see ESI†). Thus, it is likely that the decreased interdiffusion distance between reagent streams in the fast inert oil flow-focused geometry leads to faster mixing, which in turn constrains the nucleation burst, resulting in less polydisperse particles.[10]

To further illustrate the importance of the flow-focused reaction on the microfluidic platform, a batch reaction was run for comparative purposes. The solutions of $HAuCl_4$ (1 mL, 10 mM) and 1-methylimidazole (1 mL, ~4.9 M) were mixed together and stirred for 15 min. With rapid vortex mixing, 3 mL of the inert oil and 1 mL of the $NaBH_4$ solution (100 mM) were injected into the gold solution in rapid succession. In an attempt to reproduce the very short residence time in the microfluidic device (*i.e.*, 19 s), the product was collected as quickly as possible and precipitated with an equal volume of ethanol, as before. The shortest reaction time that could be achieved this way was *ca.* 1 min. When analyzed by TEM, the batch-produced AuNPs were observed to have the same general size (4.63 ± 0.76 nm; σ/μ_d = 16.4%) as those produced by microfluidic device under droplet-forming conditions; however, their polydispersity increased (see ESI†). They were also less spherical than those produced under the most optimal microfluidic conditions, with 20.2% having a roundness less than 0.85. This result serves to emphasize the benefit that

microfluidic devices provide by affording precise control over reactions parameters, such as reaction time, which is not possible in traditional batch reactions.

The approach described here compares favorably to previous microfluidic schemes for AuNP formation. Wagner and co-workers observed a similar dependence of polydispersity on mixing rate in a system based on reduction of gold salts, but the nanoparticles they produced tended to be morphologically diverse and more polydisperse than those observed here.[2c,11] Other groups have used micromixers for fast reagent mixing; however, the resulting AuNPs still tend to exhibit spheroidal morphologies and/or relatively large polydispersities.[12] The high quality of the nanoparticles fabricated here is likely due to the particle-stabilizing effects of the IL solvent working in conjunction with the controlled and fast mixing from the microfluidic device.

In conclusion, AuNPs can be prepared quickly and reproducibly in a simple PDMS microfluidic device using BMIM-BF_4. Both the size and morphological fidelity of the AuNPs can be controlled by flow focusing with an inert carrier oil. High flow rates of the inert carrier oil induce droplet formation, which result in the fabrication of monodisperse, spherical AuNPs in a matter of seconds—a result that cannot be reproduced under different flow regimes. Through control of reaction parameters, such as mixing rate in the microfluidic device and type of imidazolium-based IL, this technology should be translatable to the fabrication of other high quality nanoparticles.

Acknowledgements

This material is based on work supported by the National Science Foundation under CMMI-0926969. This work was also supported by financial assistance from the James H. Zumberge Research and Innovation Fund at USC.

References

1 (*a*) C.-H. Chang, B. K. Paul, V. T. Remcho, S. Atre and J. E. Hutchison, *J. Nanopart. Res.*, 2008, **10**, 965; (*b*) Y. Song, J. Hormes and C. S. S. R. Kumar, *Small*, 2008, **4**, 698.
2 (*a*) Y. Song, H. Modrow, L. L. Henry, C. K. Saw, E. E. Doomes, V. Palshin, J. Hormes and C. S. S. R. Kumar, *Chem. Mater.*, 2006, **18**, 2817; (*b*) E. M. Chan, R. A. Mathies and A. P. Alivisatos, *Nano Lett.*, 2003, **3**, 199; (*c*) J. Wagner and J. M. Köhler, *Nano Lett.*, 2005, **5**, 685; (*d*) S. A. Khan, A. Günther, M. A. Schmidt and K. F. Jensen, *Langmuir*, 2004, **20**, 8604; (*e*) S. Krishnadasan, R. J. C. Brown, A. J. deMello and J. C. deMello, *Lab Chip*, 2007, **7**, 1434.
3 A. J. deMello, *Nature*, 2006, **442**, 394.
4 (*a*) M. -C. Daniel and D. Astruc, *Chem. Rev.*, 2004, **104**, 293; (*b*) C. J. Murphy, T. K. Sau, A. M. Gole, C. J. Orendorff, J. Gao, L. Gou, S. E. Hunyadi and T. Li, *J. Phys. Chem. B*, 2005, **109**, 13857; (*c*) M. A. El-Sayed, *Acc. Chem. Res.*, 2001, **34**, 257.
5 M. Brust, M. Walker, D. Bethell, D. J. Schiffrin and R. Whyman, *J. Chem. Soc., Chem. Commun.*, 1994, 801.
6 J. Dupont and J. D. Scholten, *Chem. Soc. Rev.*, 2010, **39**, 1780.
7 J. N. Lee, C. Park and G. M. Whitesides, *Anal. Chem.*, 2003, **75**, 6544.
8 (*a*) P. Dash and R. W. J. Scott, *Chem. Commun.*, 2009, 812; (*b*) E. Redel, M. Walter, R. Thomann, C. Vollmer, L. Hussein, H. Scherer, M. Krüger and C. Janiak, *Chem.–Eur. J.*, 2009, **15**, 10047; (*c*) V. Khare, Z. Li, A. Mantion, A. A. Ayi, S. Sonkaria, A. Voelkl, A. F. Thünemann and A. Taubert, *J. Mater. Chem.*, 2010, **20**, 1332; (*d*) H. J. Ryu, L. Sanchez, H. A. Keul, A. Raj and M. R. Bockstaller, *Angew. Chem., Int. Ed.*, 2008, **47**, 7639; (*e*) L. Zhao, C. Zhang, L. Zhuo, Y. Zhang and J. Y. Ying, *J. Am. Chem. Soc.*, 2008, **130**, 12586; (*f*) H. Itoh, K. Naka and Y. Chujo, *J. Am. Chem. Soc.*, 2004, **126**, 3026.
9 S. K. Ghosh and T. Pal, *Chem. Rev.*, 2007, **107**, 4797.
10 J. deMello and A. deMello, *Lab Chip*, 2004, **4**, 11N.
11 J. Wagner, T. R. Tshikhudo and J. M. Köhler, *Chem. Eng. J.*, 2008, **135S**, S104.
12 (*a*) S.-Y. Yang, F.-Y. Cheng, C.-S. Yeh and G.-B. Lee, *Microfluid. Nanofluid.*, 2010, **8**, 303; (*b*) D. Shalom, R. C. R. Wootton, R. F. Winkle, B. F. Cottam, R. Vilar, A. J. deMello and C. P. Wilde, *Mater. Lett.*, 2007, **61**, 1146.